



1 **Under a new light: validation of eddy covariance flux with light response functions of**
2 **assimilation and estimates of heterotrophic soil respiration.**

3 **Georgia R. Koerber¹, Wayne, S. Meyer¹, Qiaoqi SUN¹, Peter Cale², Cacilia M. Ewenz^{3,4}**

4 ¹Department of Ecology and Environmental Science, School of Biological Sciences, The
5 University of Adelaide, Adelaide, SA 5005, Australia

6 ²Australian Landscape Trust, Riverland, Calperum Station, PO Box 955, SA 5341, Australia

7 ³CSIRO Oceans and Atmosphere Flagship, Yarralumla, ACT 2600, Australia

8 ⁴Airborne Research Australia / Flinders University, PO Box 335, SA 5106, Australia

9

10 *Correspondence to:* G.R. Koerber (georgia.koerber@adelaide.edu.au)

11

12 **Keywords:** ecosystem respiration, light response, autotrophic respiration, assimilation,
13 heterotrophic soil respiration, leaf area index, semi-arid woodland, basal soil respiration,
14 bushfire

15 **Type of Paper:** Primary Research Article

16 **Abstract.** Estimation of the basal or heterotrophic soil respiration is crucial for determination
17 of whether an ecosystem is emitting or sequestering carbon. A severe bushfire in January
18 2014 at the Calperum flux tower, operational since August 2010, provided variation in
19 ecosystem respiration and leaf area index as the ecosystem recovered. We propose ecosystem
20 respiration is a function of leaf area index and the y-intercept is an estimate of heterotrophic
21 soil respiration. We calculated an assimilation rate from eddy covariance data for light
22 response functions to calculate ecosystem respiration incorporating suppression of the
23 daytime autotrophic respiration. Ecosystem respiration from light response functions
24 correlated with data processing calculations of ecosystem respiration by OzFluxQC ($y_0 =$
25 $0.161x + 0.0085$; Adj. $r^2 = 0.698$). The relationship between ecosystem respiration and leaf
26 area index ($y_0 = 1.43x + 0.398$; Adj. $r^2 = 0.395$) was also apparent. When this approach was
27 compared to field measurements of soil respiration and mass balance calculations from
28 destructive leaf area, leaf area index calculations and litter fall, the year of data corresponding



29 to the year of soil respiration measurements, the y-intercept was $0.432 \mu\text{mol m}^{-2} \text{s}^{-1}$ or 163.44
30 $\text{gC m}^{-2} \text{year}^{-1}$ ($y_0 = 1.37x + 0.432$, Adj. $r^2 = 0.325$). The mass balance approach for the net
31 primary productivity when subtracted from the tower NEE estimated heterotrophic soil
32 respiration of $134.59 \text{gC m}^{-2} \text{year}^{-1}$. This is only 28.9gC different, therefore the y-intercept
33 approach indeed provides an estimate of heterotrophic soil respiration.

34

35 **1 Introduction**

36

37 The flux of CO_2 determined from eddy covariance (EC) measures and calculations is
38 a net value because sequestration by photosynthesising vegetation and emission from
39 respiration within a soil plant ecosystem occurs concurrently. The total of this flux over a day
40 is called the net ecosystem exchange (NEE). Partitioning EC determined NEE to quantify the
41 contributions of sequestration and emission of CO_2 is challenging. Ideally, independent
42 measures of both daytime and night-time ecosystem respiration are needed to make reliable
43 estimates of net ecosystem productivity (NEP), the amount of C retained in the ecosystem.
44 However, very few independent measures of respiration are made and so other methods of
45 estimation are used. This paper describes one approach to improve the estimate of NEP.

46 At night when photosynthesis is not occurring, the flux of CO_2 from the ecosystem
47 into the atmosphere is the measure of ecosystem respiration. However the often calm night-
48 time atmospheric conditions are not ideal for measures of CO_2 flux to and from an ecosystem.
49 Quality EC measures depend on adequate mixing of the atmosphere moving over the soil
50 plant system. This is generally not an issue during daylight hours when near surface
51 atmospheric mixing is usually large (Burba 2013). During the night however, air within the
52 vegetation layer cools and decouples from the layer of air above the plant canopy. With little
53 turbulent mixing, sensors at the top of the EC tower do not fully indicate near surface fluxes.
54 When this happens the estimate of night time CO_2 flux will be an unreliable measure of
55 ecosystem respiration (ER). To minimise the bias that this measurement limitation may
56 induce in full day exchange values, various data filters are applied. Most commonly,
57 minimum thresholds for average half hourly values of friction velocity, u^* (Goulden et al.,
58 1996) are used for removing measurements when it is deemed that there is insufficient
59 mixing. Van Gorsel et al. (2007) identified a maximum value of CO_2 flux in the early evening
60 as the appropriate value for night-time respiration at their undulating site. This may not be an



61 appropriate or reliable method for flat to moderate topography sites.

62 In the absence of independent measures or estimates of ER, many researchers
63 extrapolate from night-time CO₂ flux into the daytime (Gilmanov et al., 2007; Lasslop et al.
64 2010; Wohlfhardt et al., 2005; Reichstein et al., 2005). However it is known that daylight
65 suppresses autotrophic respiration (Heskel et al., 2013) and hence application of night-time
66 derived respiration estimates during the daytime, will lead to an underestimate of plant C
67 sequestration, often referred to as net primary production (NPP). The reason why foliar
68 autotrophic respiration in the light is suppressed compared to respiration in the night is not
69 completely understood (Ayub et al., 2014). Not with standing this, developing improved
70 methods of estimating ER is important. To assist with this it is important to recognise that ER
71 is deemed to be the sum of two components – heterotrophic (HR) and autotrophic respiration
72 (AR). Autotrophic respiration is the efflux of CO₂ emanating from otherwise
73 photosynthesising organisms that fix C while heterotrophic respiration is the efflux of CO₂
74 from all organisms that derive the C from other sources. Soil respiration has an efflux of CO₂
75 from living plant roots (autotrophic) and from a plethora of soil organisms (heterotrophic)
76 occurring concurrently. Kuzyakov and Larionova (2005) concluded that the main reasons
77 why NEE and NEP are often not equal is that the C input into the rhizosphere (part of the
78 below ground carbon (BGC) when estimating NPP) is ignored and often there is no
79 accounting or limited accounting of HR.

80 Estimates of HR have been made from extrapolation of linear regressions between
81 total soil respiration and root biomass back to the y-intercept value i.e. at zero root mass
82 (Koeber et al., 2010; Kuzyakov, 2006; Kucera and Kirkham, 1971). The causal link between
83 LAI and ER is self-evident (Xu et al., 2004; Lindroth et al., 2008; Cleverly et al., 2013) and
84 we propose that another method of deriving an estimate of HR is to extrapolate this function
85 to the y-intercept with LAI = 0. However to quantify this relationship there needs to be
86 variation in both ecosystem respiration and leaf area index, preferably with a wide range of
87 both values to establish a robust relationship. In this study a wide range of LAI resulted from
88 measurements made before and after the woodland ecosystem was burned in a bushfire.

89 The procedure used in this study to develop an improved estimate of ER and in turn
90 HR was as follows. Daylight CO₂ flux values from half hourly EC measures were adjusted by
91 subtracting an estimate of ER derived from the immediately preceding night-time flux values.
92 The ratios of associated daytime to night-time soil temperature and daytime to night-time soil
93 water content were used to scale the expected increased respiration as daytime temperatures
94 were generally greater and soil water contents slightly lower than those at night. The adjusted



95 daytime CO₂ flux was an estimate of ecosystem assimilation (A , $\mu\text{mol m}^{-2} \text{s}^{-1}$). Then the
96 relationship between A and photosynthetically active radiation (PAR, $\mu\text{mol m}^{-2} \text{s}^{-1}$), more
97 generally known as light response functions (Cleverly et al., 2013; Wohlfahrt et al., 2005;
98 Lasslop et al., 2010), for each month was plotted. The use of A instead of NEE (Gilmanov et
99 al., 2007; Lasslop et al. 2010; Wohlfahrt et al., 2005) in the light response function is an
100 attempt to account for suppression of the daytime AR by light (Heskel et al., 2013; Kok,
101 1949; Kok, 1956). The relationship between A and PAR fits a rectangular hyperbola function
102 that then enables extrapolation to PAR = 0 and hence an estimate of night-time ER.

103 The research null hypotheses of this paper are: (i) Ecosystem respiration will not be a
104 function of leaf area index. (ii) Direct night-time respiration and respiration in the night
105 derived from light response functions (using daytime data) will not correlate with each other
106 and (iii) HR from NEE + NPP will not agree with HR estimated as a y-intercept from ER
107 versus LAI.

108

109 2 Materials and methods

110

111 2.1 Site description and tower instrumentation

112 The flux monitoring site was a semi-arid mallee woodland on Calperum Station
113 approximately 20 km from Renmark in South Australia (34°00.163S, 140°35.261E; Fluxnet
114 site abbreviation: AU-Cpr). A 20m high EC tower, as part of the OzFlux Terrestrial
115 Ecosystem Research Network (TERN) was erected in June 2010 (Flight Bros. Adelaide SA)
116 and measurements began August 2010. The surrounding mallee ecosystem (Noble and
117 Bradstock, 1989) is typical of semi-arid ecosystems, adapted to long term annual median
118 rainfall (242 mm) encompassing drought years (Meyer, et al., 2015) and survives by
119 accessing occasionally replenished water stores deep in the soil profile (Mitchell et al., 2009).
120 The characteristic sand hills of the region run west to east with rolling undulations from
121 swale to crest of 5 to 8 m. The area has the largest (>1 million hectares), continuous remnant
122 of mallee habitat in Australia (Nulsen et al., 1986). Mallee surrounds the tower at least 10 km
123 in every direction. The sand hills are stabilized by eucalypt species (*Eucalyptus Dumosa*,
124 *Eucalyptus incrassata*, *Eucalyptus oleosa* and *Eucalyptus socialis*) with sparse plants of
125 *Eremophila*, *Hakea*, *Olearia*, *Senna* and *Melaleuca* genera in the mid-storey and *Triodia spp.*
126 in the understorey.



127 The mean air temperature is 25 °C (data accessed from <http://www.bom.gov.au/>) with
128 hot summers including days with maximum temperatures greater than 40 °C. The area often
129 experiences significant summer rainfall events of 20-60 mm in November to March after
130 lengthy dry periods during the year. Soils are alkaline sand (94% sand, 4% silt and 2% clay)
131 with an Australian classification of Tenosol (Isbell, 2002) and US Soil Taxonomy
132 classification of Aridisol (Soil Survey Staff, 1996). Total organic carbon, nitrogen and
133 carbonate (0-300 mm) are 0.5%, 0.04% and 0.25% respectively. Additional site detail and
134 soil properties are given in Sun et al., (submitted) and Sun et al., (2015).

135 The site experienced a bushfire during 15 to 19 January 2014 burning 52 713 ha with
136 a perimeter of 140 km according to the Country Fire Service, South Australia. The majority
137 of instruments on the OzFlux tower were destroyed by the fire. These were restored within
138 three months to monitor ecosystem recovery. A detailed description of the EC and ancillary
139 instrumentation is in Meyer et al. (2015). Briefly, measurements of three-dimensional wind
140 speed (CSAT3 sonic anemometer, Campbell Scientific Inc., Logan, UT, USA), virtual
141 temperature (CSAT3), water vapour density in air and CO₂ density in air using an open-path
142 IRGA (Licor LI7500, LiCor Biosciences, Lincoln, NE, USA), were recorded at a frequency
143 of 10 Hz.

144 Auxiliary observations of solar irradiance (Es), air temperature, vapour pressure
145 deficit (D) and rainfall, soil temperature and soil water content were also collected
146 concurrently. Incident Es was observed from a four component radiometer that was
147 positioned at a height of 20 m (CNR4, Kipp and Zonen, Delft, the Netherlands). D was
148 determined as the difference between atmospheric vapour pressure (kPa) and saturation
149 vapour pressure at air temperature (HMP45C, Vaisala, Helsinki, Finland) at a height of 2 m.
150 An additional pyranometer (Licor LI2003S, LiCor Biosciences, Lincoln, NE, USA) was
151 mounted at 20 m and cup anemometers and wind direction sensors (RM Young, Traverse
152 City MI, USA) at 2 and 8.6 m. Onsite rainfall (CS7000, Hydrologic services, Warwick,
153 NSW, Australia) was measured with the tipping bucket gauge (0.2 mm resolution) mounted
154 on a stand of height 0.65 m in a clear area 8 m from the tower. Soil temperature and water
155 content sensors (CS650, Campbell Scientific, Townsville, Australia) were buried 10 metres
156 away from the tower base with multiple depths, ranging from 0.1 m to 1.8 m. Sensors were
157 placed in bare soil (inter-canopy) or beneath eucalypt canopies (under canopy). The collars
158 for measuring soil respiration in burnt Mallee were within 200 m from the tower base.

159 Covariances were computed every 30 min to generate fluxes following standard data
160 processing and quality assurance and correction procedures (Isaac et al., (In preparation for



161 this Special Issue); Cleverly et al., 2013; Eamus et al., 2013), hereafter referred to as
162 OzFluxQC. A friction coefficient (u^*) threshold was then calculated and set to 0.26 m s^{-1} ,
163 0.21 m s^{-1} , 0.23 m s^{-1} , 0.25 m s^{-1} , 0.26 m s^{-1} and 0.26 m s^{-1} for the years 2010, 2011, 2012,
164 2013, 2014 and 2015 respectively.

165 To calculate the effective sampling footprint of the tower we used the Kormann-
166 Meixner method (Kormann and Meixner, 2001), employing a modified version of the ART
167 Footprint Tool of Neftel et al. (2008). The Kormann-Meixner footprint determines the two-
168 dimensional density function for an ellipse upwind from the tower. The predominant wind
169 direction here is from the south-westerly quarter. For every 30 minute measurement of wind
170 speed and direction, mixing and buoyancy parameters the data is filtered according to the
171 Kormann-Meixner constraints. Analysis of the seasonal effects exhibited a smaller footprint
172 in summer which reflected the increased mixing in summer as well as the influence of more
173 frequent winds from the northerly quarter. The annual average of the footprint area for 2014
174 displayed a distance from the tower of 500 m for at least 10% of the maximum contribution
175 (1300 m for at least 1%).

176 The regression of latent energy plus sensible heat ($LE + H$) against net radiation plus
177 soil heat flux ($R_n + G$) was used to check energy balance closure. From 1 August 2010 to 31
178 August 2013 the relationship was $(LE + H) = 0.8769 (R_n + G) + 2.5095$, $r^2 = 0.9159$. This
179 indicated that energy balance was not completely achieved, as is commonly observed with
180 the eddy covariance method (Twine et al., 2000).

181

182 2.2 Light response functions

183 The light response function needed was the relationship between the assimilation rate
184 (A) and the incoming radiant energy. Assimilation was partitioned from NEE as shown in the
185 schematic flow chart (Fig. 1). To calculate A from NEE the daytime values of NEE were
186 increased in absolute magnitude by the expected rate of CO_2 emission from the soil and plant
187 system. The daily night-time 30 minute respiration ($AR + HR$) values were adjusted using the
188 ratio of average daytime soil temperature to the night-time soil temperature. A further,
189 generally minor adjustment was made using the ratio of average daytime to night-time soil
190 water content measured at 100 mm depth. The adjusted night-time average value was then
191 subtracted from each daytime 30 minute flux to give an assimilation (A) rate with an absolute
192 value greater than NEE. The calculation of A for every 30 minutes of the daytime in each
193 month was then regressed against short wave radiant energy converted to photosynthetically



194 active radiation (PAR) in $\mu\text{mol m}^{-2} \text{s}^{-1}$ according to Meek et al., (1984) and McCree (1972) as
 195 detailed in Biggs (1984).

196 A rectangular hyperbola was fitted to the 30 minute data each month (Eqn. 1,
 197 Wohlfahrt et al., 2005; Lasslop et al., 2010; Cleverly et al., 2013) with starting values of -10,
 198 300 and 0.5 for the net saturated A (V_{max}), saturating PAR (K_m) and constant (c) respectively,
 199 all in $\mu\text{mol m}^{-2} \text{s}^{-1}$. The value of A when PAR = 0 was assigned as the night-time respiration
 200 (R_{night}) value for that month. Further, rearranging the same equation and solving for the value
 201 of PAR when A = 0 (Eqn. 2) gave the compensation point when low PAR and hence
 202 photosynthesis no longer compensated respiration (Heskel et al., 2013). When PAR was
 203 greater than this compensation point, ER was deemed to be suppressed by the incoming
 204 radiant energy.

205

$$206 \quad A = V_{\text{max}} \times (\text{PAR} / (K_m + \text{PAR})) + c \quad \text{Eqn. 1}$$

207

208 Where V_{max} is the light saturated net photosynthetic rate

209 K_m is the saturation light intensity

210 c is a constant

211

$$212 \quad \text{PAR} = (K_m (A - c)) / (V_{\text{max}} - A + c) \quad A = 0 \quad \text{Eqn. 2}$$

213

214 Fitting the rectangular hyperbola model used the SPSS procedure (IBM SPSS Statistics V. 21
 215 New York, US) of nonlinear weighted least squares fitting using the Levenberg-Marquardt
 216 algorithm.

217

218 2.3 Leaf area index

219 During May 2013 to September 2015, plant area index (PAI) of the canopy above 0.5 m from
 220 the ground was measured optically using the digital cover photography method (DCP) (Pekin
 221 and Macfarlane, 2009, Macfarlane et al., 2007) as described in Eamus et al., (2013). A 1 ha
 222 (100 m x 100 m) area immediately to the north west of the tower was marked and 10 x 100 m
 223 transects were identified along which photographs were taken at 10 m intervals. Photographs
 224 were taken using a Sony Nex-7 DSLR camera fitted with a lens of 25 mm focal length. The
 225 camera settings were automatic exposure, aperture-priority mode, F-stop of 9.0 and ISO 400.
 226 The camera was oriented to 0° nadir (viewing upward). Calculation of PAI used an extinction



227 coefficient of 0.5. For eight months after the fire the photographs taken were of the trunks
228 and branches without leaves. This area could be subtracted from the previously determined
229 plant area to obtain LAI.

230 For cross calibration purposes leaf area was determined directly by destructively
231 collecting epicormic stem and leaf regrowth of five trees in April 2015, approximately one
232 year after the bushfire. Leaves from a stem were removed, and a subsample of leaves was
233 measured with a leaf area meter. The subsample and main leaf sample were weighed after
234 oven drying at 60°C for 48 hours, and the specific leaf area of the subsample was used to
235 calculate the whole tree leaf area.

236

237 **2.4 Soil respiration, litter collection, tree spacing and biomass**

238 Soil CO₂ efflux was measured monthly from July 2014 to June 2015 (total 12 sampling
239 campaigns) with a manual chamber connected to an infra-red gas analyser (LI-8100, LI-COR
240 Inc., Lincoln, Nebraska, USA). Details are in Sun et al., (accepted May 2016).

241 In May 2013, 3 litter trays (450 × 340 × 55 mm aluminium BBQ trays) were placed in
242 the 1 ha area adjacent to the tower. These were dug in and secured so that the upper edge was
243 flush with the ground surface. Litter was collected monthly, dried at 60 °C for 48 hours and
244 weighed. The carbon content was assumed to be 35% of plant material dry mass (Hadley and
245 Causton, 1984).

246 On 17 June 2014 remnant (burnt) tree trunks within the 1 ha area adjacent to the tower
247 were viewed aurally, without the obstruction of any leaf canopy using a 3D Robotics RTF
248 Y6 conservation drone. Images were captured at 70 metres above ground at a resolution of
249 21.6 mm per pixel in RGB colour. Images were mosaicked with Pix4Dmapper and improved
250 by referencing to an existing ortho-rectified aerial photographic image. The central point of
251 each mallee tree was marked with a digital dot while viewing the imagery at scale of 1:100 in
252 ArcGIS. The mean distance between trees could then be calculated and this spacing used to
253 scale up biomass and LAI from the sub sample measurements.

254 The total carbon associated with the 1 ha area was estimated from the measurements
255 of tree numbers and dry mass of eight destructively sampled trees. This enabled an estimate
256 of aboveground carbon (AGC). An estimate of belowground carbon (BGC) was made using
257 soil respiration measurements and litter amounts (Koerber et al., 2009; Clark et al., 2001;
258 Raich and Nadellhoffer, 1989; Nadellhoffer et al., 1998).

259



260 **3 Results**

261

262 The results were determined primarily from the light response functions and the extrapolated
263 values of respiration in the night from daytime A. These values reflect the environmental
264 conditions the mallee ecosystem was experiencing each month of a year.

265

266 **3.1 Net ecosystem exchange**

267

268 During the four years prior to 2010, the annual average rainfall was 215 mm, with
269 each year being consistently below the long term median annual rainfall of 242 mm. These
270 dry years were part of a prolonged dry period generally referred to as the “Millennium
271 drought”. Significant rain (259 mm) fell in the last five months of 2010, the Millennium
272 drought ended and the mallee ecosystem became a C sink with monthly NEE of -15.49 g C
273 $\text{m}^{-2} \text{ month}^{-1}$ for December 2010. During 2011, with further rain (511 mm for the year) the
274 mallee responded and recovered as indicated by an increase in NEE to $-25.70 \text{ g C m}^{-2} \text{ month}^{-1}$
275 for July 2011 and a maximum of $-44.46 \text{ g C m}^{-2} \text{ month}^{-1}$ in April 2011. This increased uptake
276 of C corresponded to an observed increase in green leaf canopy of both trees and grass cover
277 that was reflected in increased remotely sensed NDVI values and inferred LAI back
278 calculated from latent energy exchange determined by the EC measurements (Meyer et al.
279 2015). This response is consistent with the wide area response during March to May 2011 of
280 Australian arid and semi-arid vegetation to the summer rainfall of 2010 – 2011 (Poulter et al.,
281 2014; Cleverly et al., 2016). During 2012, the recovered ecosystem was sustained during the
282 first half of the year with maximum NEE of $-42.83 \text{ g C m}^{-2} \text{ month}^{-1}$ in April 2012. The
283 second half of 2012 was dry (62 mm of rain) and this lower than average rainfall continued
284 into most of 2013. In 2013 the maximum NEE was only $-17.82 \text{ g C m}^{-2} \text{ month}^{-1}$ in August.
285 This rate is similar to that recorded at the end of the Millennium drought in late 2010. In
286 January 2014 the destruction of the vegetation in the bushfire resulted in the ecosystem
287 becoming a carbon source, with a maximum emission of $13.53 \text{ g C m}^{-2} \text{ month}^{-1}$ recorded in
288 May 2014. Signs of vegetation recovery were evident in July 2014 as the mallee trees
289 sprouted epicormic stems and juvenile leaves from the lignotubers. In the months of August
290 and September 2014, NEE was -7.73 and $-7.59 \text{ g C m}^{-2} \text{ month}^{-1}$ respectively. In 2015, the
291 ecosystem was a sink with a maximum NEE of $-20.75 \text{ g C m}^{-2} \text{ month}^{-1}$ in June. Annual NEE
292 from OzFluxQC for each year along with the partitioning into gross primary productivity
293 (GPP) and ER are given in Table 1.



294

295 3.2 Assimilation light response functions

296

297 The half hourly assimilation (A) values and associated radiation (PAR) values for each month
298 of the entire measurement period were plotted and the assimilation light response function
299 fitted (Table 2). In the summer of 2012, throughout 2013, and the spring and summer of
300 2015, when the mallee ecosystem was dry, regression r^2 were higher with PAR threshold <
301 $1500 \mu\text{mol m}^{-2} \text{s}^{-1}$. Even so the regressions had higher coefficients during the winter months
302 and were lower in summer months. This likely indicates that assimilation was more
303 constrained by available radiation in the cooler, less evaporative winter months, while in
304 summer, assimilation was constrained by greater stomatal control as water availability to
305 meet high evaporative demand was limiting (Ayub et al., 2011; Meyer et al., 2015).

306 The relationship between night-time respiration, derived from the flux tower
307 measurements using OzFluxQC processing against night-time respiration determined
308 indirectly from the y-intercept of daytime A and PAR response functions (Fig. 2) are
309 significantly correlated and approximately similar in the years preceding the bushfire
310 although 2013 was experiencing drought (Pearson correlations, 2010: $r = 0.873$, $P \leq 0.05$;
311 2011: $r = 0.58$, $P \leq 0.05$; 2012: $r = 0.615$, $P \leq 0.05$; 2013: $r = 0.27$, $P = 0.396$, Fig. 2). In 2014
312 after the bushfire, all values were small ($< 0.7 \mu\text{mol m}^{-2} \text{s}^{-1}$) with the flux tower values
313 generally being larger than those derived from the light response functions. In 2015, night-
314 time respiration from the tower and from light response curves continued to be small. The
315 spread of respiration values determined from the assimilation light response function is
316 similar in 2014 and 2015 but was smaller than those estimated in the years before the
317 bushfire.

318

319 3.3 Comparison of ER from (NEE – A) and ER from OzFluxQC

320 Calculation of ER as (NEE – A) was significantly correlated to ER from the
321 processing by OzFluxQC, Pearson $r = 0.838$ $P \leq 0.0001$ (Fig. 3). From the equation of the
322 line ($y_0 = 0.1612x + 0.0085$, $r^2 = 0.6977$), the OzFluxQC is underestimating ER with smaller
323 positive rates compared to ER from a calculated A. The larger positive ER corresponds to a
324 more negative ER if using the convention of negative rates for respiration (Atkin et al., 2013)
325 and is in line with their statements that not incorporating suppressed daytime respiration
326 underestimates ER.



327

328 3.4 Relationship between ER and LAI and estimates of HR

329 The relationship between ER derived from ($NEE - A$) and LAI for 25 months around the
330 bushfire was highly significant (Fig. 4; $y_0 = 1.43x + 0.398$; Adj. $r^2 = 0.395$, Pearson
331 correlation, $r = 0.648$ $P \leq 0.0001$). From this relation the inferred ER for this period is 0.398
332 $\mu\text{mol m}^{-2} \text{s}^{-1}$. The ecosystem respiration was standardized to 20 °C and 0.03 g g⁻¹ soil water
333 content to remove seasonal variation. There are three outlier points with apparently
334 suppressed ER for the months of April, May and June 2014, immediately after the bushfire.
335 For the period from July 2014 to June 2015 that corresponds to the year that in-situ soil
336 respiration measurements were made post fire, the y-intercept is 0.4316 $\mu\text{mol m}^{-2} \text{s}^{-1}$ ($y_0 =$
337 $1.365x + 0.4316$, Adj. $r^2 = 0.3249$, Pearson correlation $r = 0.570$ $P = 0.053$). The value at LAI
338 = 0 gave an estimate of ER and more particularly HR of 163.44 gC m⁻² year⁻¹.

339 An alternative approach to estimate HR is to calculate the sum of AGC and BGC, that
340 is effectively net primary production (NPP), and subtract OzFluxQC derived NEE. Using the
341 mean ground area per tree of 16 m² derived from drone imagery, the annual increase in AGC
342 was estimated to be 105.68 ± 27.37 gC m⁻² year⁻¹. For July 2014 to June 2015, soil
343 respiration was estimated to be 490.72 gC m⁻² (details in Sun et al., 2016), litter fall was
344 566.17 ± 62.57 gC m⁻² and hence BCG was 75.45 gC m⁻² year⁻¹. The sum of AGC and BGC
345 and therefore NPP is 181.13 gC m⁻² year⁻¹. With NEE for the year of $-46.54 \pm$ gC m⁻² year⁻¹
346 the estimate of HR is 134.59 gC m⁻². This compares very favourably with the estimate
347 (163.44 gC m⁻²) from light response functions and is 44% of NEE. This coincidence indicates
348 that the method of extrapolation of the assimilation (A) and incoming energy (PAR)
349 relationship to PAR = 0 (i.e. the y-intercept) provides an estimate of ER each month
350 incorporating AR.

351

352 4 Discussion

353

354 In this paper we have demonstrated another way to partition NEE recorded by EC
355 towers into the C sequestered by photosynthesis and the efflux of C from respiration.
356 Calculation of daily NEP using an estimate of ER from extrapolation of ecosystem light
357 response functions using A instead of NEE, indicates that derived NEP is inevitably larger
358 i.e. the NEE light response function usually overestimates daily respiration (Ayub et al.,



359 2011; Heskell et al., 2013). The method of estimating HR from the extrapolation of the ER
360 (NEE-A) versus LAI, is similar to that of estimating HR from the y-intercept of soil
361 respiration and root mass (Koerber et al., 2010; Kuzyakov, 2006; Kucera and Kirkham,
362 1971). The concept of the y-intercept providing an estimate of heterotrophic soil respiration
363 from the assimilation light response function is novel and hasn't been used to assist
364 partitioning EC derived NEE.

365 The estimates for HR of $163.44 \text{ gC m}^{-2} \text{ year}^{-1}$ from light response function derived ER
366 versus LAI or $134.59 \text{ gC m}^{-2} \text{ year}^{-1}$ from (NEE + NPP) are equivalent to $1.63 \text{ tC ha}^{-1} \text{ year}^{-1}$
367 and $1.34 \text{ tC ha}^{-1} \text{ year}^{-1}$ respectively. As expected, these are lower but of the same order of
368 magnitude as that estimated ($8.13 \text{ tC ha}^{-1} \text{ year}^{-1}$) in much wetter and more plant productive
369 vegetable farming regions in the UK (Koerber et al., 2009).

370 Partitioning of NEE derived from EC measurements indicates that in semi-arid
371 environments, the timing of rainfall relative to preceding drying greatly influences the
372 outcome of the dynamic balance between sequestration and respiration. For example, Xu et
373 al. (2004) found that in a Mediterranean grassland the early onset of rain in the winter
374 growing season resulted in C assimilation i.e. gross primary productivity (GPP) to be greater
375 than ER and NEE was negative i.e. the ecosystem was a carbon sink. However if significant
376 rainfall did not occur until late in spring or early summer and the water stressed grass was
377 dead, ER was greater than GPP and NEE was positive i.e. the ecosystem was a carbon source.
378 Monthly values of NEP and ER derived in this study suggest that the timing of rainfall in
379 relation to the preceding dry or wet period was more important in determining the net C
380 balance of the ecosystem than the total amount over the course of a year. Paul Jarvis's
381 research (Jarvis et al., 2007) on soil respiration pulses after rain, carrying on the discovery by
382 H.F. Birch 50 years ago (the "Birch" effect) showed the same effect. His research and that of
383 Xin Wang et al (2014) suggests that increased rainfall in summer, along with increasing
384 ambient temperature from global warming will increase the contribution of HR in soil
385 respiration. Soil respiration pulses following rainfall may be enhanced by the availability of
386 organic breakdown materials coming from photo-degradation during drought periods (Ma et
387 al., 2012). Rainfall that irregularly occurs in persistently arid areas such as the *Corymbia*
388 savanna and Mulga ecosystems of inland Australia seems to cause net carbon loss at least in
389 the short term (Cleverly et al., 2016).

390 The relationship between direct and indirect derived night-time respiration shown in
391 Fig. 2 was close to 1:1 during 2010 and 2011. Drying in 2012 persisted into 2013 and this
392 seems to have affected this relationship. With the bushfire in 2014 there was no active



393 photosynthetic canopy and only a small but increasing amount in 2015, the amount of
394 respiration declined presumably because both AR and HR declined – AR because the
395 majority of the above ground growth was dead and HR because there is no supply or little
396 supply of photosynthetically derived C from the above ground system to below ground. The
397 reasons why EC estimates of night-time respiration in 2014 appear to be large relative to the
398 light response function is uncertain. With loss of the tree, mid story and ground canopy the
399 atmospheric exchange and mixing would be different. It is not clear why this may cause what
400 appears to be an over-estimate of the CO₂ flux. However it is equally possible that the light
401 response functions are underestimating the flux since active leaf area is very low and hence
402 assimilation is very limited.

403 After careful consideration, two more problems had to be reconciled. The first is
404 calculations of assimilation were an underestimate in the outset. With ER equilibrated in the
405 night and the day from a ratio of the soil temperature and soil water content in the night and
406 the day, subsequent subtraction covers over some of the A seen as respiration in the day is in
407 fact suppressed (Heskel et al., 2013). For example if ER was constant in the night and the day
408 at 3 μmol m⁻²s⁻¹ and the photosynthetic rate is -8 μmol m⁻²s⁻¹, when the night is subtracted
409 away from the day we are left with an assimilation of -2 μmol m⁻²s⁻¹ however if ER is 1 μmol
410 m⁻²s⁻¹ in the day then assimilation will be -4 μmol m⁻²s⁻¹. Therefore we had an assimilation
411 rate that was an underestimate. In the future we aim to develop methods for conducting linear
412 regressions to estimate autotrophic respiration in the daylight (Heskel et al., 2013; Kok, 1949;
413 Kok, 1956) for correcting the underestimate of A (Koerber et al., unpublished).

414 The second problem is whether our calculations of A require correction like *in vivo*
415 construction of light response functions requiring A versus CO₂ partial pressure (p_i) curves at
416 three low light intensities (Villar et al., 1994; Kirschbaum and Farquhar, 1987). As p_i is
417 increased at low light intensity, measurements of A increase. Therefore p_i should be
418 standardized for all light intensities and A adjusted to ensure foliar AR provides a correct
419 estimate of the Kok effect and hence A is not an overestimate. Our tower measurements
420 provided multiple A estimates at each light intensity with an external CO₂ partial pressure
421 that was reasonably constant. With this setting the EC derived light response functions do not
422 require standardization.

423

424 5 Conclusion

425

426 The advantage of using the light response function approach to determine respiration



427 when $PAR = 0$ is that it is non-destructive. The ecosystem remains intact, soils are not
428 disturbed and there is no need to measure respiration of the plants directly with all of the
429 attendant problems of sufficient sampling to assure representativeness. In this study we did
430 field measurements that were destructive but only to the extent of AGC necessary for the
431 NPP. The BGC was estimated from litter collections and soil respiration. This study
432 highlights the importance of measuring soil respiration as an adjunct measurement.

433 The similarity in heterotrophic soil respiration estimated by field measurements and
434 from the determination of assimilation from partitioning the NEE as described here is
435 encouraging, only 28.85 gC m^{-2} difference. This result indicates that the NEE and NEP are
436 balanced at our site and we did not underestimate NEP from our field measurements. From
437 our initial calculations, our measurements provide rarely available evidence of the large
438 contribution of basal soil respiration (44%) to the total C balance. Management of the land by
439 land use managers needs to minimize the formation of ecosystems susceptible to larger
440 emissions of basal soil respiration arising from our changing climate. There is much to gain
441 from understanding dry and arid ecosystem functioning of the plants within the sandy
442 alkaline soils of southern Australia. Mallee's are an important biomass crop, potentially
443 providing an increasing income from payments for carbon sequestration, for landholders.

444 This study has been able to reject all three null hypotheses. When the hypotheses are
445 addressed in reverse order, firstly, we were able to estimate the heterotrophic soil respiration
446 from field measurements and the y-intercept of ecosystem respiration versus leaf area index.
447 Secondly, light use efficiency functions for the respiration in the dark from rectangular
448 hyperbola agree with direct night time data. Lastly, ecosystem respiration is a function of
449 LAI.

450

451

452

453

454

455

456

457

458

459



460 **Table 1.** Annual GPP, ER, NEE in $\text{gC m}^{-2} \text{ year}^{-1}$ and rainfall for 2011 to 2015. Values are
461 from OzFluxQC. Measurements started at the tower in August 2010 and GPP, ER, NEE and
462 rainfall are sums for August to December 2010 (5 months).

463

Year	GPP	ER	NEE	Rainfall mm
2010	100.74	29.84	-70.9	259.0
2011	432.05	114.37	-317.68	510.8
2012	377.84	93.68	-284.16	211.2
2013	237.15	68.73	-168.41	242.4
2014	52.03	32.57	-19.46	211.6
2015	155.02	56.55	-98.47	241.4

464

465

466

467

468

469

470

471

472

473

474

475

476

477

478

479

480

481

482

483



484 **Table 2.** Coefficients from assimilation light response functions. Units are $\mu\text{mol m}^{-2} \text{s}^{-1}$.
 485 Rainfall in brackets is from Renmark when the EC measurement system was not in operation
 486 after bushfire.

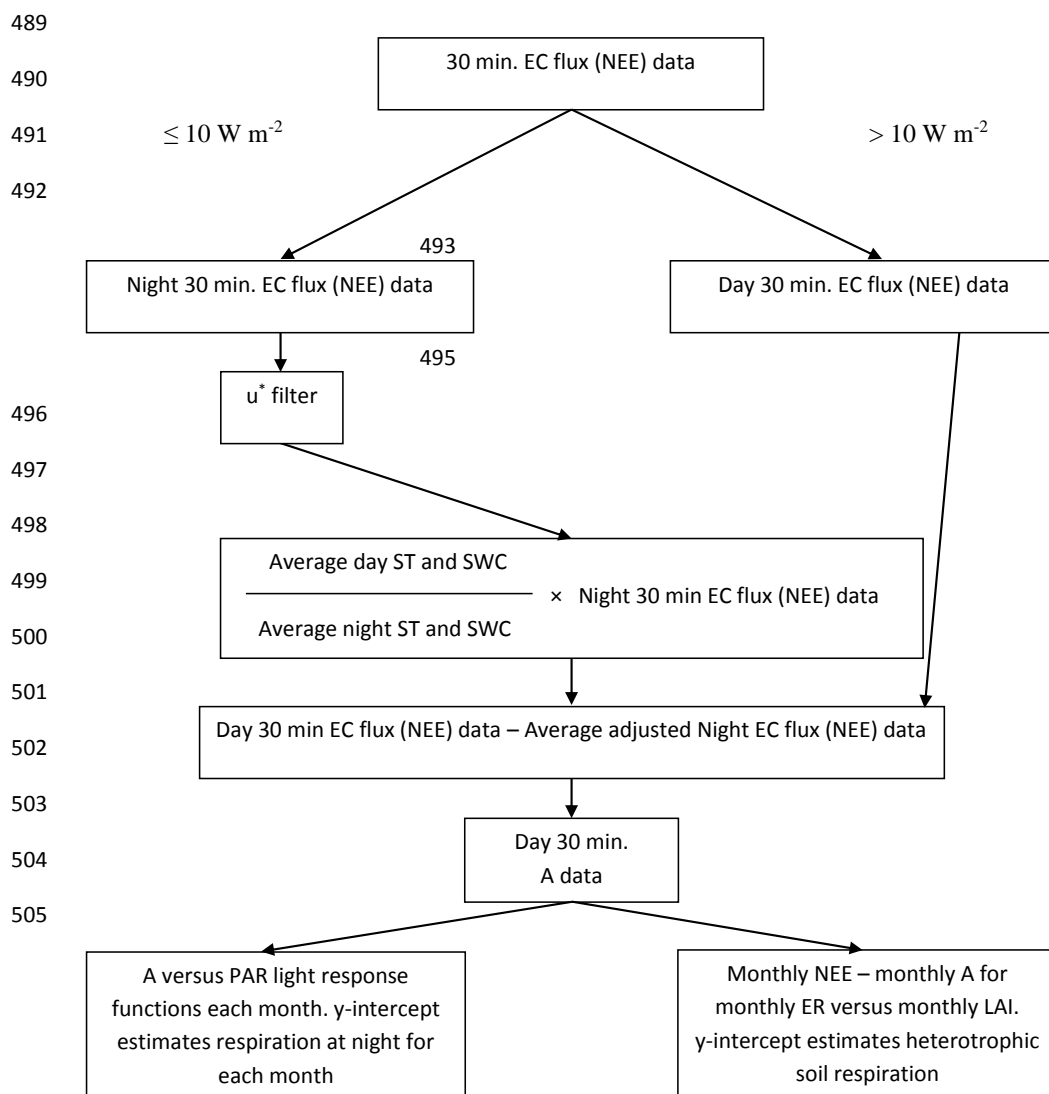
	Rainfall mm	Compensation point when $F_c = 0$	Vmax	Km	ER in night , r^2 and n from rectangular hyperbola
Units are all $\mu\text{mol m}^{-2} \text{s}^{-1}$					
2010					
July	6.0	76.3	-3.2	456.8	0.47 $r^2=0.74$ $n=25$
August	24.0	96.5	-3.9	392.8	0.78 $r^2=0.41$ $n=520$
September	48.0	110.2	-4.5	558.3	0.74 $r^2=0.40$ $n=565$
October	67.0	140.8	-4.7	825.5	0.68 $r^2=0.26$ $n=633$
November	35.0	160.4	-4.4	331.4	1.44 $r^2=0.28$ $n=615$
December	86.0	115.3	-4.8	316.5	1.28 $r^2=0.25$ $n=749$
2011					
January	87.4	135.5	-7.3	577.9	1.39 $r^2=0.36$ $n=743$
February	109.0	153.4	-9.9	522.9	2.24 $r^2=0.46$ $n=604$
March	63.4	114.7	-12.1	887.6	1.39 $r^2=0.61$ $n=613$
April	4.4	73.3	-12.1	1024.0	0.81 $r^2=0.52$ $n=541$
May	14.2	86.4	-11.2	576.3	1.46 $r^2=0.52$ $n=445$
June	4.8	72.7	-9.7	647.3	0.98 $r^2=0.61$ $n=459$
July	13.4	85.7	-7.8	493.2	1.15 $r^2=0.56$ $n=497$
August	25.0	102.0	-7.6	492.7	1.30 $r^2=0.38$ $n=510$
September	8.2	108.9	-5.7	460.5	1.09 $r^2=0.28$ $n=577$
October	29.8	99.4	-5.0	316.8	1.20 $r^2=0.26$ $n=656$
November	59.4	166.2	-5.6	515.8	1.37 $r^2=0.29$ $n=667$
December	91.8	98.4	-6.8	793.0	0.75 $r^2=0.27$ $n=769$
2012					
January	27.4	122.7	-7.0	423.9	1.56 $r^2=0.40$ $n=777$
February	86.8	85.7	-5.8	689.1	1.65 $r^2=0.24$ $n=657$
March	9.4	150.7	-10.4	215.5	1.86 $r^2=0.49$ $n=643$
April	5.4	86.7	-9.0	456.9	1.44 $r^2=0.36$ $n=550$
May	9.0	86.5	-8.8	380.6	1.64 $r^2=0.52$ $n=503$
June	11.0	89.3	-10.3	743.7	1.10 $r^2=0.61$ $n=452$
July	23.6	109.5	-9.3	753.2	1.18 $r^2=0.56$ $n=485$
August	8.2	89.2	-8.6	743.5	0.92 $r^2=0.64$ $n=571$
September	5.8	96.2	-6.1	353.2	1.31 $r^2=0.14$ $n=488$
October	3.8	88.6	-4.7	626.5	0.59 $r^2=0.15$ $n=445$
November	14.0	65.1	-3.5	222.7	0.79 $r^2=0.29$ $n=432$
December	6.8	61.8	-4.8	726.1	0.38 $r^2=0.22$ $n=318$



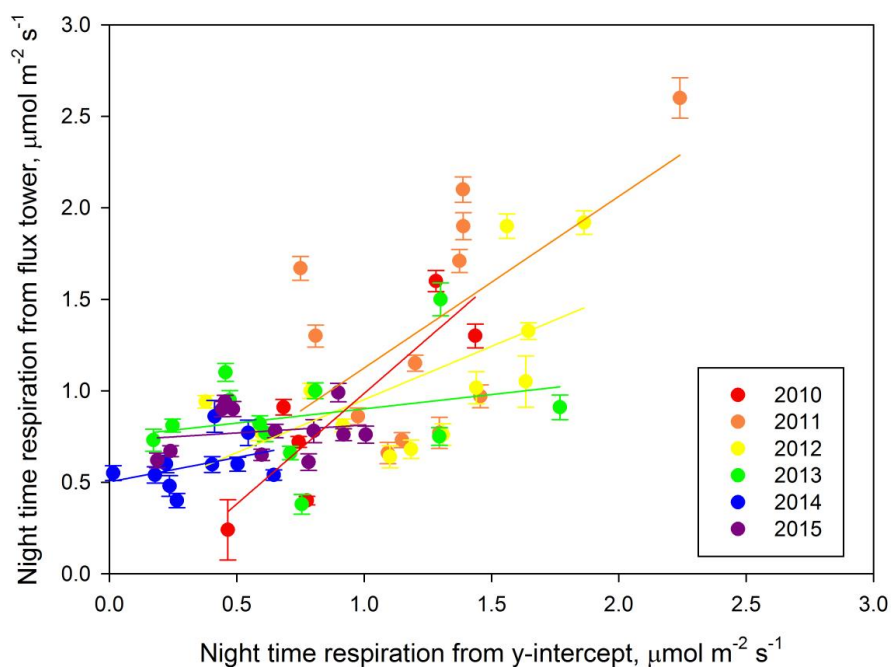
2013					
January	1.0	44.1	-3.7	613.6	0.25 $r^2=0.14$ $n=305$
February	36.8	105.0	-3.9	772.8	0.47 $r^2=0.08$ $n=275$
March	2.2	184.9	-7.6	1065.8	1.12 $r^2=0.31$ $n=465$
April	13.6	48.3	-10.5	1578.7	0.81 $r^2=0.31$ $n=266$
May	35.4	81.8	-6.5	1792.4	0.61 $r^2=0.39$ $n=208$
June	32.0	138.3	-9.7	617.5	1.77 $r^2=0.63$ $n=275$
July	24.4	88.1	-10.8	1249.5	0.71 $r^2=0.60$ $n=392$
August	10.6	90.8	-9.5	1045.7	0.78 $r^2=0.58$ $n=353$
September	26.2	160.4	-6.0	578.3	1.30 $r^2=0.30$ $n=396$
October	9.2	60.2	-4.0	350.7	0.59 $r^2=0.24$ $n=221$
November	3.6	23.6	-3.9	508.1	0.17 $r^2=0.14$ $n=435$
December	27.2	46.3	-3.8	339.0	0.46 $r^2=0.16$ $n=303$
2014					
January	(6.8)	45.8	-5.2	1087.1	0.41 $r^2=0.14$ $n=165$
February	(84.4)				
March	(15.0)				
April	(35.6)	-1695.8	-0.4	532.1	0.55 $r^2=0.00$ $n=66$
May	28.4	-0.8	0.7	39.8	0.02 $r^2=0.01$ $n=334$
June	13.8	2364.7	-1.0	1371.1	0.65 $r^2=0.02$ $n=368$
July	4.6	333.3	-1.0	1204.0	0.22 $r^2=0.02$ $n=382$
August	18.8	131.6	-4.2	1973.6	0.27 $r^2=0.23$ $n=477$
September	6.6	89.4	-2.8	1331.1	0.18 $r^2=0.12$ $n=317$
October	0.6	92.3	-1.4	171.4	0.50 $r^2=0.06$ $n=618$
November	9.2	95.5	-1.2	378.4	0.24 $r^2=0.03$ $n=686$
December	13.8	135.6	-2.0	520.8	0.40 $r^2=0.08$ $n=696$
2015					
January	68.8	104.4	-2.9	584.1	0.44 $r^2=0.30$ $n=722$
February	0.6	93.0	-2.7	459.3	0.45 $r^2=0.21$ $n=378$
March	0.0	106.2	-2.1	271.2	0.60 $r^2=0.16$ $n=420$
April	65.4	129.3	-2.7	411.3	0.65 $r^2=0.20$ $n=448$
May	9.8	97.2	-6.8	638.2	0.90 $r^2=0.61$ $n=376$
June	17.8	80.7	-7.5	671.4	0.80 $r^2=0.38$ $n=280$
July	6.0	84.7	-6.0	562.0	0.78 $r^2=0.57$ $n=362$
August	20.4	110.7	-5.8	524.6	1.01 $r^2=0.41$ $n=469$
September	17.0	102.8	-4.2	368.5	0.92 $r^2=0.28$ $n=561$
October	1.5	16.3	-3.4	2480.4	0.02 $r^2=0.08$ $n=232$
November	23.0	21.0	-2.4	774.2	0.06 $r^2=0.10$ $n=419$
December	0.0	91.4	-1.6	661.5	0.19 $r^2=0.07$ $n=419$

487

488



514 **Figure 1.** Schematic flow chart showing the method for partitioning carbon fluxes.



515

516 **Figure 2.** Night respiration from the EC tower measurement system and the y-intercept
517 approach with daytime data.

518 2010: $y_0 = 1.20x - 0.22$ Adj. $r^2 = 0.7617$

519 2011: $y_0 = 0.94x + 0.19$ Adj. $r^2 = 0.34$

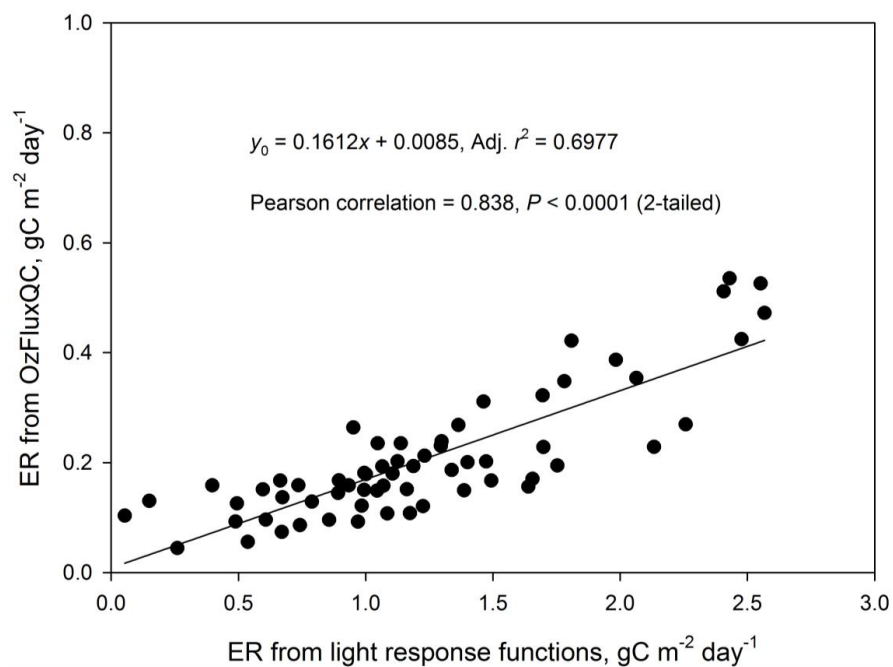
520 2012: $y_0 = 0.58x + 0.37$ Adj. $r^2 = 0.3783$

521 2013: $y_0 = 0.16x + 0.75$ Adj. $r^2 = 0.07$

522 2014: $y_0 = 0.27x + 0.50$ Adj. $r^2 = 0.1477$

523 2015: $y_0 = 0.09x + 0.73$ Adj. $r^2 = 0.0312$

524



525

526

527 **Figure 3.** Comparison of ecosystem respiration from the OzFluxQC processing and the light

528 response function of calculated assimilation.

529

530

531

532

533

534

535

536

537

538

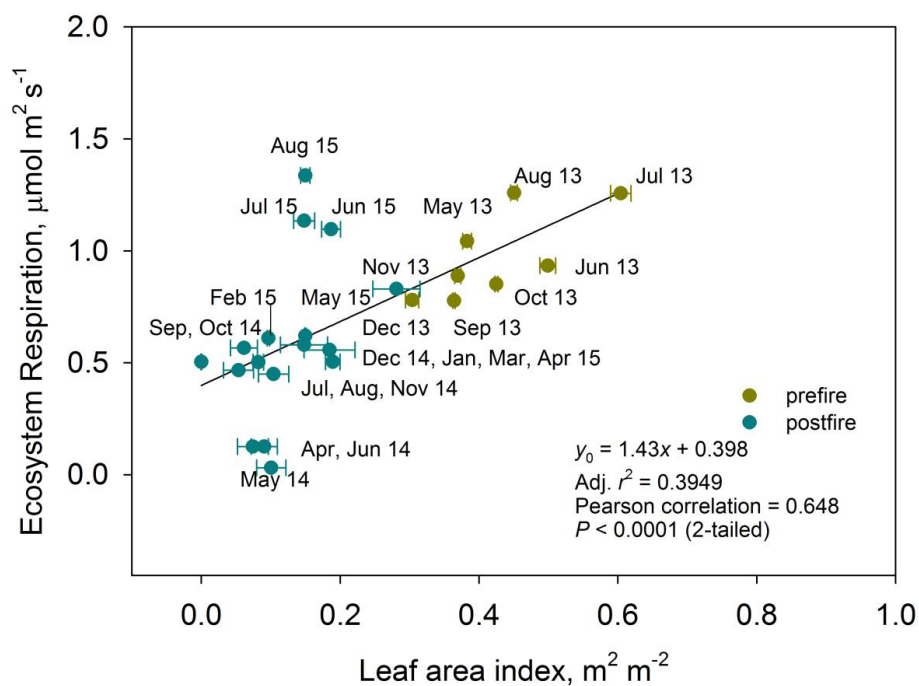
539

540

541

542

543



544
 545 **Figure 4.** Comparison of ecosystem respiration from the light response function with
 546 calculated assimilation extrapolated to LAI = 0 and LAI from digital cover photography. The
 547 ecosystem respiration was standardized to 20 °C and 0.03 g g⁻¹ soil water content.

548
 549
 550
 551
 552
 553
 554
 555
 556
 557
 558
 559
 560



561 *Author contributions.* G.R. Koerber and W.S. Meyer designed the experiment and carried it
562 out. G.R. Koerber, P. Cale, Q. Sun, W.S. Meyer and C. M. Ewenz performed field work.
563 G.R. Koerber, W.S. Meyer and C. M. Ewenz performed data collection and processing. G.R.
564 Koerber and W.S. Meyer prepared the manuscript with contributions from all co-authors.

565

566 *Acknowledgements.* This work was partly supported by grants from the Australian
567 government's Terrestrial Ecosystems Research Network (TERN) (www.tern.org.au). TERN
568 is a research infrastructure facility established under the National Collaborative Research
569 Infrastructure Strategy (NCRIS) and Education Infrastructure Fund, Super Science Initiative,
570 through the Department of Industry, Innovation, Science, Research, and Tertiary Education.
571 Thank you to 12 National Australia Bank employees under the support and expert guidance
572 of Cassandra Collins from the Earthwatch Institute and Peter Cale from the Riverland
573 Australian Landscape Trust.

574

575 **References**

576

577 Atkin, O. K.; Turnbull, M. H.; Zaragoza-castells, J.; Fyllas, N. M.; Lloyd, J.; Meir, P.;
578 Griffin, K. L.: Light inhibition of leaf respiration as soil fertility declines along a post-glacial
579 chronosequence in New Zealand: an analysis using the Kok method, *Plant and Soil*, 367, 163-
580 182, doi: 10.1007/s11104-013-1686-0, 2013.

581

582 Ayub, G., Smith, R., Tissue, D.T., and Atkin, O.K.: Impacts of drought on leaf respiration in
583 darkness and in the light in *Eucalyptus saligna* exposed to industrial-age atmospheric CO₂
584 and growth temperature, *New Phytologist*, 190, 1003–1018, doi: 10.1111/j.1469-
585 8137.2011.03673.x, 2011.

586

587 Ayub, G., Zaragoza-Castells, J., Griffin, K.L., Atkin, O.K.: Leaf respiration in darkness and
588 in the light under pre-industrial, current and elevated atmospheric CO₂ concentrations, *Plant*
589 *Science*, 226, 120-130, doi: 10.1016/j.plantsci.2014.05.001, 2014.

590

591 Biggs, W.W.: Principles of Radiation Measurement. Li-cor report. Excerpted from:
592 Advanced Agricultural Instrumentation. Proceedings from the NATO Advanced Study
593 Institute on "Advanced Agricultural Instrumentation", edited by: W.G. Gensler, Martinus
594 Nijhoff Publishers, Dordrecht, The Netherlands, 1984.



595
596 Bréda, N.J.J.: Ground-based measurements of leaf area index: a review of methods,
597 instruments and current controversies, *Journal of Experimental Botany*, 54, 2403-2417, doi:
598 10.1093/jxb/erg263, 2003.
599
600 Bruhn, D., Mikkelsen, T.N., Herbst, M., Kutsch, W.L., Ball, M.C., and Pilegaard, K.:
601 Estimating daytime ecosystem respiration from eddy-flux data, *Biosystems*, 103, 309–313,
602 doi: 10.1016/j.biosystems.2010.10.007, 2011.
603
604 Clark, D.A., Brown, S., Kicklighter, D.W., Chambers, J.Q., Thomlinson, J.R., and Ni, J.:
605 Measuring net primary production in forests: concepts and field methods, *Ecological*
606 *Applications*, 11, 356–370, doi: 10.1890/1051-0761, 2001.
607
608 Cleverly, J., Eamus, D., Van Gorsel, E., Chen, C., Rumman, R., Luo, Q., Restrepo Coupe, N.,
609 Li, L., Kljun, N., Faux, R., Yu, Q., Huete, R.: Productivity and evapotranspiration of two
610 contrasting semiarid ecosystems following the 2011 global carbon land sink anomaly,
611 *Agricultural and Forest Meteorology*, 220, 151-159, doi: 10.1016/j.agrformet.2016.01.086,
612 2016.
613
614 Cleverly, J., Boulain, N., Villalobos-Vega, R., Grant, N., Faux, R., Wood, C., Cook, P.G.,
615 Yu, Q., Leigh, A., and Eamus, D.: Dynamics of component carbon fluxes in a semi-arid
616 *Acacia* woodland, central Australia, *Journal of Geophysical Research*, 118, 1168-1185, doi:
617 10.1002/jgrg.20101, 2013.
618
619 Eamus, D., Cleverly, J., Boulain, N., Grant, N., Faux, R., and Villalobos, V.R.: Carbon and
620 water fluxes in an arid-zone *Acacia* savanna woodland: analyses of seasonal patterns and
621 responses to rainfall events, *Agricultural and Forest Meteorology*, 182-183, 225-238, doi:
622 10.1016/j.agrformet.2013.04.020, 2013.
623
624 Gilmanov, T.G., Soussana, J.F., Aires, L., Allard, V., Ammann, C., Balzarolo, M., Barcza, Z.,
625 Bernhofer, C., Campbell, C.L., Cernusca, A., Cescatti, A., Clifton-Brown, J., Dirks, B.O.M.,
626 Dore, S., Eugster, W., Fuhrer, J., Gimeno, C., Gruenwald, T., Haszpra, L., Hensen, A., Ibrom,
627 A., Jacobs, A.F.G., Jones, M.B., Lanigan, G., Laurila, T., Lohila, A., Manca, G., Marcolla,
628 B., Nagy, Z., Pilegaard, K., Pinter, K., Pio, C., Raschi, A., Rogiers, N., Sanz, M.J., Stefani,



- 629 P., Sutton, M., Tuba, Z., Valentini, R., Williams, M.L., and Wohlfahrt, G.: Partitioning
630 European grassland net ecosystem CO₂ exchange into gross primary productivity and
631 ecosystem respiration using light response function analysis, *Agriculture, Ecosystems &*
632 *Environment*, 121, 93–120, doi: 10.1016/j.agee.2006.12.008, 2007.
- 633
- 634 Goulden, M. L., Munger, J.W., Fan, S. M., Daube, B. C. and Wofsy, S. C.: Measurements of
635 carbon sequestration by longterm eddy covariance: methods and a critical evaluation of
636 accuracy, *Global Change Biology*, 2, 169–182, doi: 10.1111/j.1365-2486.1996.tb00070.x,
637 1996.
- 638
- 639 Hadley, P. and Causton, D.R.: Changes in percentage organic-carbon content during
640 ontogeny, *Planta*, 160, 97-101, doi: 10.1007/BF00392856, 1984.
- 641
- 642 Heskell, M.A., Atkin, O.K., Turnbull, M.H., and Griffin, K.L.: Bringing the Kok effect to
643 light: A review on the integration of daytime respiration and net ecosystem exchange, 4, 1-
644 14, doi: 10.1890/ES13-00120.1, 2013.
- 645
- 646 Isaac, P.R., Cleverly, J., Beringer, J., McHugh, I.: The OzFlux network data path: from
647 collection to curation, In preparation for this Special Issue, *Biogeosciences*, 2015.
- 648
- 649 Isbell, R.: *The Australian soil classification*, Melbourne, Australia, CSIRO publishing, 1986.
- 650
- 651 Jarvis, P., Rey, A., Petsikos, C., Wingate, L., Rayment, M., Pereira, J., Banza, J., David, J.,
652 Miglietta, F., Borghetti, M., Manca, G., Valentini, R.: Drying and wetting of Mediterranean
653 soils stimulates decomposition and carbon dioxide emission: the “Birch effect” *Tree*
654 *Physiology* 27, 929–940, doi: 10.1093/treephys/27.7.929, 2007.
- 655
- 656 Koerber, G.R., Edwards-Jones, G., Hill, P.W., Milà i Canals, L., Nyeko, P., York, E.H., and
657 Jones, D.L.: Geographical variation in carbon dioxide fluxes from soils in agro-ecosystems
658 and its implications for life-cycle assessment, *Journal of Applied Ecology*, 46, 306–314, doi:
659 10.1111/j.1365-2664.2009.01622.x, 2009.
- 660
- 661 Koerber, G.R., Hill, P.W., Edwards-Jones, G., and Jones, D.L.: Estimating the component of
662 soil respiration not dependent on living plant roots: Comparison of the indirect y-intercept



- 663 regression approach and direct bare plot approach, *Soil Biology and Biochemistry*, 42, 1835-
664 1841, doi: 10.1016/j.soilbio.2010.06.024, 2010.
- 665
- 666 Kok, B.: On the interrelation of respiration and photosynthesis in green plants, *Biochimica et*
667 *Biophysica Acta*, 3, 625–631, doi:10.1016/0006-3002(49)90136-5, 1949.
- 668
- 669 Kok, B.: On the inhibition of photosynthesis by intense light, *Biochimica et Biophysica Acta*,
670 21, 234–244, doi:10.1016/0006-3002(56)90003-8, 1956.
- 671
- 672 Kormann, R. and Meixner, F.X.: An analytical footprint model for non-neutral stratification,
673 *Boundary-Layer Meteorology*, 99, 207-224, doi: 10.1023/A:1018991015119, 2001.
- 674
- 675 Kucera, C.L. and Kirkham, D.R.: Soil respiration studies in Tallgrass Prairie in Missouri,
676 *Ecology*, 52, 912-915, doi: 10.2307/1936043, 1971.
- 677
- 678 Kuzyakov, Y.: Sources of CO₂ efflux from soil and review of partitioning methods, *Soil*
679 *Biology and Biochemistry*, 38, 425-448, doi:10.1016/j.soilbio.2005.08.020, 2006.
- 680
- 681 Kuzyakov, Y. and Larionova, A.A.: Root and rhizomicrobial respiration: A review of
682 approaches to estimate respiration by autotrophic and heterotrophic organisms in soil, *Journal*
683 *of Plant Nutrition and Soil Science*, 168, 503–520, doi: 10.1002/jpln.200421703, 2005.
- 684
- 685 Lasslop, G., Reichstein, M., Papale, D., Richardson, A.D., Arneth, A., Barr, A., Stoy, P., and
686 Wohlfahrt, G.: Separation of net ecosystem exchange into assimilation and respiration using a
687 light response curve approach: critical issues and global evaluation, *Global Change Biology*,
688 16, 187–208, doi: 10.1111/j.1365-2486.2009.02041.x, 2010.
- 689
- 690 Lindroth, A., Lagergren, F., Aurela, M., Bjarnadottir, B., Christensen, T., Dellwik, E., Grelle,
691 A., Ibrom, A., Johansson, T., Lankreijer, H., Launiainen, S., Laurila, T., Molder, M.,
692 Nikinmaa, E., Pilegaard, K., and Sigurdsson, B.D.: Leaf area index is the principal scaling
693 parameter for both gross photosynthesis and ecosystem respiration of Northern deciduous and
694 coniferous forests, *Tellus*, 60B, 129-142, doi: 10.1111/j.1600-0889.2007.00330.x, 2008.
- 695
- 696 Ma, S., Baldocchi, Hatala, J.A., Detto, M., Curiel Yuste, J.: Are rain-induced ecosystem



- 697 respiration pulsed enhanced by legacies of antecedent photodegradation in semi-arid
698 environments? *Agricultural and Forest Meteorology*, 154-155, 203-213, doi:
699 10.1016/j.agrformet.2011.11.007, 2012.
700
- 701 Macfarlane, C., Hoffman, M., Eamus, D., Kerp, N., Higginson, S., McMurtrie, R., and
702 Adams, M.: Estimation of leaf area index in eucalypt forest using digital photography.
703 *Agricultural and Forest Meteorology*, 143, 176-188, doi: 10.1016/j.agrformet.2006.10.013,
704 2007.
705
- 706 McCree, K.J.: Test of current definitions of photosynthetically active radiation against leaf
707 photosynthesis data, *Agricultural Meteorology*, 10, 443-453, doi: 10.1016/0002-
708 1571(72)90045-3, 1972.
709
- 710 Meek, D.W., Hatfield, J.L., Howell, T.A., Idso, S.B., and Reginato, R.J.: A Generalised
711 Relationship Between Photosynthetically Active Radiation and Solar Radiation, *Agronomy*
712 *Journal*, 76, 939-945, doi: 10.2134/agronj1984.00021962007600060018x, 1984.
713
- 714 Meyer, W.S., Kondrolovà, E., and Koerber, G.R.: Evaporaton of perennial semi-arid woodland
715 in southeastern Australia is adapted for irregular but common dry periods, *Hydrological*
716 *Processes*, 29, 3714-3726, doi: 10.1002/hyp.10467, 2015.
717
- 718 Mitchell, P.J., Veneklaas, Lambers, H., and Burgess, S.S.O.: Partitioning of
719 evapotranspiration in a semi-arid eucalypt woodland in south-western Australia, *Agricultural*
720 *and Forest Meteorology*, 149, 25-37, doi: 10.1016/j.agrformet.2008.07.008, 2009.
721
- 722 Nadelhoffer, K.J., Raich, J.W., and Aber, J.D.: A global trend in belowground carbon
723 allocation: comment, *Ecology*, 79, 1822-1825, doi: 10.2307/176802, 1998.
724
- 725 Neftel, A., Spirig, C., and Ammann, C.: Application and test of a simple tool for operational
726 footprint evaluations, *Environmental Pollution*, 152, 644-652,
727 doi:10.1016/j.envpol.2007.06.062, 2008.
728
- 729 Noble, J.C. and Bradstock, R.A.: An historical overview of ecological studies, Ch. 1. In
730 *Mediterranean Landscapes in Australia: Mallee Ecosystems and their Management*, Noble,



- 731 J.C., Bradstock, R.A. (eds). CSIRO: East Melbourne.
732
- 733 Nulsen, R.A., Bligh, K.J., Baxter, I.N., Solin, E.J., and Imrie, D.H.: The fate of rainfall in a
734 mallee and heath vegetated catchment in South Western Australia, *Australian Journal of*
735 *Ecology*, 11, 361-371, doi: 10.1111/j.1442-9993.1986.tb01406.x, 1986.
736
- 737 Pekin, B. and Macfarlane, C.: Measurement of Crown Cover and Leaf Area Index Using
738 Digital Cover Photography and Its Application to Remote Sensing, *Remote Sensing*, 1, 1298-
739 1320, doi:10.3390/rs1041298, 2009.
740
- 741 Poulter, B., Frank, D., Ciais, P., Myneni, R.B., Andela, N., Bi, J., Broquet, G., Canadell, J.G.,
742 Chevallier, F., Liu, Y.Y., Running, S.W., Sitch, S., and van der Werf, G.R.: Contribution of
743 semi-arid ecosystems to interannual variability of the global carbon cycle, *Nature*, 509, 600-
744 604, doi:10.1038/nature13376, 2014.
745
- 746 Raich, J.W. and Nadelhoffer, K.J.: Belowground carbon allocation in forest ecosystems:
747 global trend, *Ecology*, 70, 1346–1354, doi: 10.2307/1938194, 1989.
748
- 749 Reichstein, M., Falge, E., Baldocchi, D., Papale, D., Aubinet, M., Berbigier, P., Bernhofer,
750 C., Buchmann, N., Gilmanov, T., Granier, A., Grünwald, Havránková, K., Ilvesniemi, H.,
751 Janous, D., Knohl, A., Laurila, T., Lohila, A., Loustau, D., Matteucci, G., Meyers, T.,
752 Miglietta, F., Ourcival, J-M., Pumpanen, J., Rambal, S., Rotenberg, E., Sanz, M., Tenhunen,
753 J., Seufert, G., Vaccari, F., Vesala, T., Yakir, D., and Valentini, R.: On the separation of net
754 ecosystem exchange into assimilation and ecosystem respiration: review and improved
755 algorithm, *Global Change Biology*, 11, 1424-1439, doi: 10.1111/j.1365-2486.2005.001002.x,
756 2005.
757
- 758 Soil Survey Staff.: *Keys to Soil Taxonomy* 7th Edition, US Department of Agriculture, Natural
759 Resources Conservation Service, 1996.
760
- 761 Sun, Q., Meyer, W.S., Koerber, G.R., and Marschner, P.: Response of respiration and nutrient
762 availability to drying and rewetting in soil from a semi-arid woodland depends on vegetation
763 patch and a recent wildfire, *Biogeosciences*, 12, 5093-5101, doi: 10.5194/bg-12-5093-2015,
764 2015.



765

766 Sun, Q., Meyer, W.S., Koerber, G.R. and Marschner, P.: A wildfire event influences
767 ecosystem carbon fluxes but not soil respiration in a semi-arid woodland, *Agricultural,
768 Forestry and Meteorology*, doi:10.1016/j.agrformet.2016.05.019, 2016.

769

770 Twine, T.E., Kustas, W.P., Norman, J.M., Cook, D.R., Houser, P.R., Meyers, T.P., Prueger,
771 J.H., Starks, P.J., and Wesely, M.L.: Correcting eddy-covariance flux underestimates over a
772 grassland, *Agricultural and Forest Meteorology*, 103, 279–300, doi: PII: S0168-
773 1923(00)00123-4, 2000.

774

775 van Gorsel, E., Leuning, R., Cleugh, H.A., Keith, H., Suni, T.: Nocturnal carbon efflux:
776 reconciliation of eddy covariance and chamber measurements using an alternative to the u*-
777 threshold filtering technique, *Tellus*, 59B, 397–403, doi: 10.1111/j.1600-0889.2007.00252.x,
778 2007.

779

780 Wang, X., Liu, L., Piao, S., Janssens, I.A., Tang, J., Liui, W., Chi, Y., Wang, J., Xu, S.: Soil
781 respiration under climate warming: differential response of heterotrophic and autotrophic
782 respiration, *Global Change Biology*, 20, 3229–3237, doi: 10.1111/gcb.12620, 2014.

783

784 Wohlfahrt, G., Anfang, C., Bahn, M., Haslwanter, A., Newesely, C., Schmitt, M., Dresler,
785 M., Pfadenhauer, J., and Cernusca, A.: Quantifying nighttime ecosystem respiration of a
786 meadow using eddy covariance, chambers and modelling, *Agricultural and Forest
787 Meteorology*, 128, 141–162, doi:10.1016/j.agrformet.2004.11.003, 2005.

788

789 Xu, L. and Baldocchi, D.: Seasonal variation in carbon dioxide exchange over a
790 Mediterranean annual grassland in California, *Agricultural and Forest Meteorology*, 1232,
791 79–96, doi:10.1016/j.agrformet.2003.10.004, 2004.

792